The Effect of Grain Size on the High-Strain, High-Strain-Rate Behavior of Copper

MARC A. MEYERS, UMBERTO R. ANDRADE, and ATUL H. CHOKSHI

Copper with four widely differing grain sizes was subjected to high-strain-rate plastic deformation in a special experimental arrangement in which high shear strains of approximately 2 to 7 were generated. The adiabatic plastic deformation produced temperature rises in excess of 300 K, creating conditions favorable for dynamic recrystallization, with an attendant change in the mechanical response. Preshocking of the specimens to an amplitude of 50 GPa generated a high dislocation density; twinning was highly dependent on grain size, being profuse for the 117- and 315-μm grain-size specimens and virtually absent for the 9.5-μm grain-size specimens. This has a profound effect on the subsequent mechanical response of the specimens, with the smaller grain-size material undergoing considerably more hardening than the larger grain-size material. A rationale is proposed which leads to a prediction of the shock threshold stress for twinning as a function of grain size. The strain required for localization of plastic deformation was dependent on the combined grain size/shock-induced microstructure, with the large grain-size specimens localizing more readily. The experimental results obtained are rationalized in terms of dynamic recrystallization, and a constitutive equation is applied to the experimental results; it correctly predicts the earlier onset of localization for the large grain-size specimens. It is suggested that the grain-size dependence of shock response can significantly affect the performance of shaped charges.

I. INTRODUCTION

WHEREAS the effect of grain size on the quasistatic response of copper has been extensively studied,[1–6] its high-strain-rate response has only recently received attention. Quasistatic experiments yield flow stress–grain size relationships that can be conveniently fit into a Hall–Petch type equation, although there is substantial variation in the Hall–Petch parameters. This relationship seems to break down in the nanocrystalline region,[7] where other deformation mechanisms may become operative. Schmidt *et al.*[8] investigated the effect of grain size on the high-strain-rate deformation of copper but had a range of grain sizes that was quite narrow: 16 to 54 μm. They obtained, as the most significant effect, an increased surface roughness (after plastic deformation) for the 54-μm specimens. Gourdin and Lassila[5,6] tested copper specimens with grain sizes of 10, 50, 100, and 175 μm in the strain-rate range of 1×10^{-3} to 1×10^{2} s^{-1} and applied the mechanical threshold stress constitutive equation to the results. The flow stress at low and high strain rates clearly followed a Hall–Petch relationship, and the Hall–Petch slope was not very sensitive to strain rate. Recently, Nesterenko and co-workers[9,10] investigated the instability of plastic flow in dynamically loaded hollow copper cylinders (subjected to external loading by explosives) with grain sizes of 30, 100, and 1000 μm and found significant grain-size effects. Concurrently and independently, Andrade *et al.*[11,12] obtained similar results.

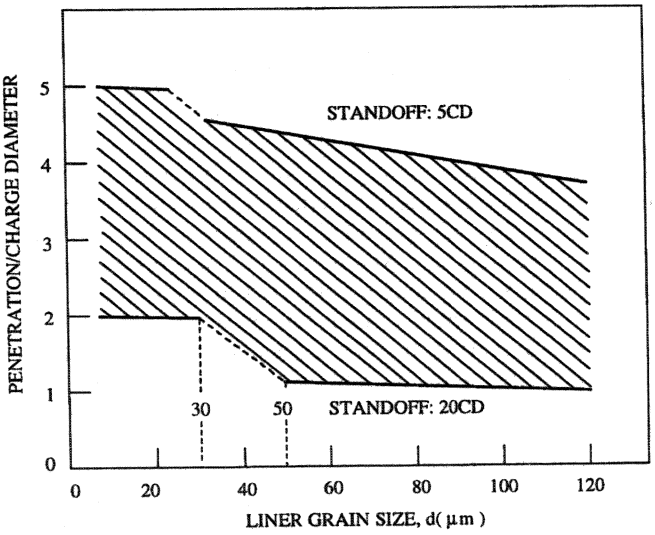

Fig. 1—Normalized penetration as a function of grain size for copper shaped charge from plot by Gurevich *et al.*,[17] based on data by Golasky.

The grain size is known to play an important role in the performance of copper shaped charges. The principle of operation of shaped charges is described by Walters and Zukas.[13] Lichtenberger *et al.*[14] investigated the behavior of shaped charge copper liners with grain sizes of 20 and 90 μm and found that the jet breakup times (related directly to the tensile ductility) were considerably higher for the 20-μm specimens. Gourdin[15,16] obtained similar results using the expanding-ring method. Tensile instability was retarded in fine-grained copper, leading to larger overall elongations. Gurevitch *et al.*[17] recently reported results by Golaski and

MARC A. MEYERS, Professor of Materials Science, is with the Department of Applied Mechanics and Engineering Sciences, University of California, San Diego, La Jolla, CA 92093-0411. UMBERTO R. ANDRADE, formerly with the Department of Applied Mechanics and Engineering Sciences, University of California, is Professor, Department of Materials Science, Military Institute of Engineering, 22290 Rio de Janeiro, Brazil. ATUL H. CHOKSHI, formerly with the Department of Applied Mechanics and Engineering Sciences, is Professor, Department of Metallurgy, Indian Institute of Science, 560012 Bangalore, India.

Manuscript submitted October 4, 1993.

Table I. Characteristics and Processing of Materials

Material	Processing	Grain Size (μm)	Composition (ppm)
Experiment 1 (plate)	Rolled down to 7 mm annealing:		
	673 K for 240 s	9.5 ± 0.3	O: 6
	773 K for 1200 s	25 ± 0.7	N: 3
	873 K for 6000 s	117 ± 2	C < 10
	1073 K for 6000 s	315 ± 12	H: 0.5
Experiment 2 (cylinder)	Cold forged down to 11-mm thick annealing:		
	673 K for 240 s	same	O: 5
	773 K for 1200 s	range as	N: 3
	873 K for 6000 s	above	C < 10
	1073 K for 6000 s		H: 0.4

Duffy, which clearly show that the penetration by shaped charges into target increases in a discontinuous manner when the grain size is reduced. Figure 1 shows these results; the ordinate axis represents the normalized penetration (penetration/charge diameter). Two standoff distances were used: 5 and 20 times charge diameter (81 mm). There is clear evidence for a significant increase in penetration as the grain size is reduced below 30 μm.

It was suggested by Meyers *et al.*[18] that direct observation of recovered shaped-charge jets and slugs may lead to inconclusive results because of the slow cooling times (on the order of seconds). On the other hand, the hat-shaped specimen provides cooling within milliseconds. Chokshi and Meyers[19] proposed that dynamic recrystallization was responsible for the extended elongation undergone by shaped-charge jets, and Andrade *et al.*[20] performed systematic experiments on copper subjected to high strains ($\gamma \sim 2 \rightarrow 5$) at high strain rates ($\sim 10^4$ s^{-1}) and demonstrated that dynamic recrystallization takes place in such a regime.

The objective of the present investigation on the dynamic response with a change in grain size was to study the underlying mechanisms responsible for these significant differences in the performance of copper. In order to simulate the environment encountered by a copper shaped charge, the specimens were preshocked to a peak pressure of 50 GPa and pulse duration of 2 μs. The shock-hardened specimens were subsequently subjected to high-strain, high-strain-rate plastic deformation in order to simulate the large strains imparted in shaped charges.

II. EXPERIMENTAL TECHNIQUES

A. *Materials*

The copper used in this investigation was acquired in the form of one plate and one cylindrical bar stock. These materials contain 99.99 pct copper, classified as oxygen-free high-conductivity. The oxygen, nitrogen, hydrogen, and carbon contents of the materials, as established from chemical analysis, are given in Table I. The impurity level has been shown[21] to have a significant effect on recrystallization kinetics. In the present research, the two coppers had a very low (less than 10 ppm) level of interstitial impurities and their compositions can be considered identical. In order to obtain various grain sizes, a series of heat treatments were conducted at 667, 773, 873, and 1173 K for annealing times of 4, 20, 60, and 100 minutes; a tube furnace with a constant flow of argon was used to protect the material from oxidation. Linear intercept grain-size measurements from the chosen conditions were performed with the help of an image processing program. For this condition, at least 400 intercepts were taken to ensure a confidence level of 95 pct and an error margin of 5 pct. Table I summarizes the cold-working and annealing procedures, as well as the average grain sizes obtained.

Assuming that d_0 is the average grain size for the initial time (t_0 = 4 minutes), one can derive an expression for the grain growth[21] as

$$d^2 - d_0^2 = s\,(t - t_0) \qquad [1]$$

where d is the grain size at time t and s is a constant of proportionality. If the diffusion of atoms across a grain boundary is considered to be a simple activated process, then s can be expressed as

$$s = s_0 \exp\left(-\frac{Q}{RT}\right) \qquad [2]$$

where s_0 is a constant, Q the activation energy for the grain growth process, T the absolute temperature, and R the gas constant. Figure 2(a) shows the experimental results in terms of grain sizes *vs* annealing times for three different temperatures; the slope of each line is the constant of proportionality, s. Figure 2(b) is an Arrhenius type plot of s *vs* $1/T$, which yielded an activation energy for grain growth of 60 ± 15 kJ mol^{-1}. Recently, Ghauri *et al.*[22] reported an activation energy for grain growth in polycrystalline copper of ~80 kJ mol^{-1}.

B. *Shock Conditioning*

The copper plate specimens were shock hardened by planar impact using an explosively accelerated flyer plate through a classical shock-loading assembly. Figure 3 shows schematically the system used. The detonator initiates a planar wave generator, which in turn simultaneously initiates the top surface of a cylindrical charge of PBX 9501. The explosive lens is designed to transform the linear detonation front into a planar shock front to the flyer plate. Therefore, the detonator transmits the front to two explosives which have different detonation velocities: the inside explosive has a detonation velocity lower than the outside one. The CETR (Center for Explosives Technology Research) plane-wave lens (30-cm diameter) using a combination of emulsion and plastic explosives was used. The explosive charge accelerates a flyer plate (4.7-mm-thick stainless steel) which impacts the system containing the specimens. Lateral and bottom momentum traps were provided to ensure that only one compressive pulse traversed the specimen. Eight disks with four different grain sizes were inserted in a copper plate stacked into two layers. The same scheme was used in experiment 2 with the addition of a cooling recovery bath. It consisted of a plastic drum filled with water, and the specimens were cooled in a dry ice–alcohol bath at 277 K prior to shocking. This ensured a lowering of the residual temperature by ~30 K, as well as an immediate

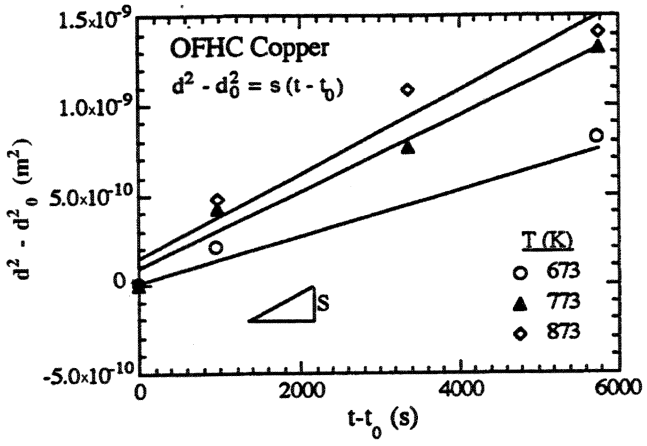

(*a*)

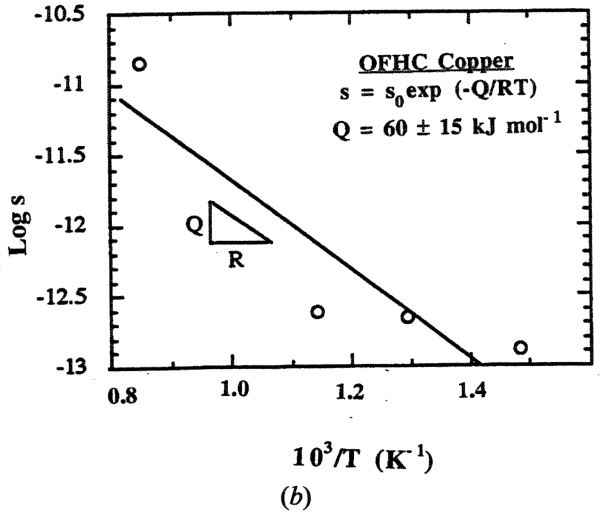

(*b*)

Fig. 2—Graphical determination of the activation energy of grain growth: (*a*) plot of time *vs* square of grain size and (*b*) plot of log *s vs* reciprocal of the absolute temperature.

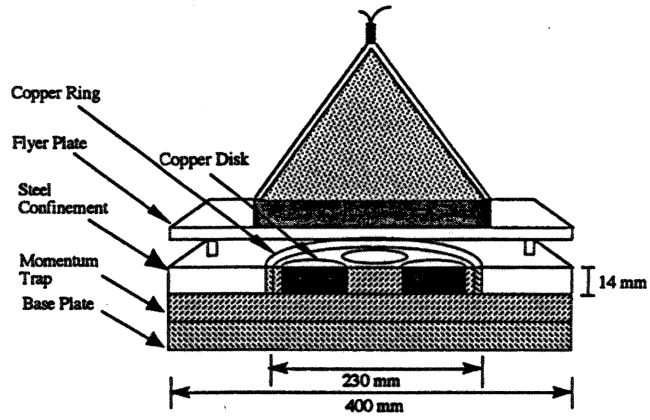

Fig. 3—Experimental setup for shock-hardening copper.

quenching of the shock-loaded specimens. Following Mogilevsky and Teplyakova's[23] suggestions, a taper angle was used in the montage of the inserts, so that the reflected waves could be laterally trapped. Therefore, lateral yielding was compensated by simultaneous pressing of the insert into the hole. A steel confinement plate was also used to decrease the lateral strain in the disks as much as possible. The result was a significant decrease in the residual strain compared to an earlier experiment;[18,20] in the present experiment, the residual strain was found to be less than 5 pct. The results obtained by Gray[24] show conclusively that residual plastic strain has a marked effect on residual microstructures.

The velocity of the flyer plate was measured by means of contact pins. Four pin assemblies were placed at different positions over the specimens, and the velocity was obtained by dividing the pin gap by the time interval. An average value was obtained using the four measured velocities. The shock pressures were determined through the equations of state of the steel flyer plate and copper target. The calculation procedure is described by DeCarli and Meyers.[25] The measured velocity in the two tests was 2.2 km s^{-1}, which corresponds to a pressure of approximately 50 GPa with an initial pulse duration of 2 μs.

C. *Mechanical Testing and Characterization*

Quasistatic compression tests were conducted in servohydraulic and screw-driven Instron machines in the strain-rate range of 10^{-4} to 10^{-1} s^{-1}. High-strain-rate tests were conducted in a split Hopkinson bar. Two tests were conducted for each condition, and three tests, if the results were not reproducible. The stress-strain curves were within ± 5 pct. In the plots presented in the next section, only one curve (characteristic) is shown for each condition. The standard deviation of the results is reflected in Figure 7. Two types of specimens were machined from the copper plates before and after the shock loading: cylindrical specimens (6-mm diameter and 6-mm long) were machined for quasistatic compression tests. For dynamic compression tests, cylindrical specimens, 6-mm diameter and 3.6-mm long, were used. The hat-shaped specimens were developed by Hartmann *et al.*[26] and Meyer and Manwaring,[27] and they can generate highly deformed regions, as shown in Figures 4(a) and (b). A spacer ring is used to limit the displacement which determines the amount of shear strain imposed on the material. The external diameter of the hat-shaped specimens was 15 mm, and other dimensions are marked on Figure 4. All specimens were prepared by electrical discharge machining (EDM) to prevent heating, which could cause changes in the unstable substructure of the shocked material. Their longitudinal axes were kept perpendicular to the plane of the plate. The shear strain was established from the ratio of the controlled displacement, δ, and the width of the shear band, λ. By geometry, the shear strain γ can be related to the uniaxial strain ε as follows:

$$\varepsilon = \ln\left(\frac{\gamma^2}{2} + \gamma + 1\right)^{1/2} \qquad [3]$$

The split Hopkinson bar used in the dynamic experiments was developed by Kolsky[28] and modified by Nemat-Nasser *et al.*,[29,30] who introduced a wave-trapping scheme enabling samples to be subjected to a simple pulse of preassigned shape and duration and then to be recovered without any additional loading.

Optical and electron microscopy were conducted in order to characterize the microstructure. Specimens for transmission electron microscopy were extracted from 3-mm-diameter EDM cylinders, containing the shear region of the

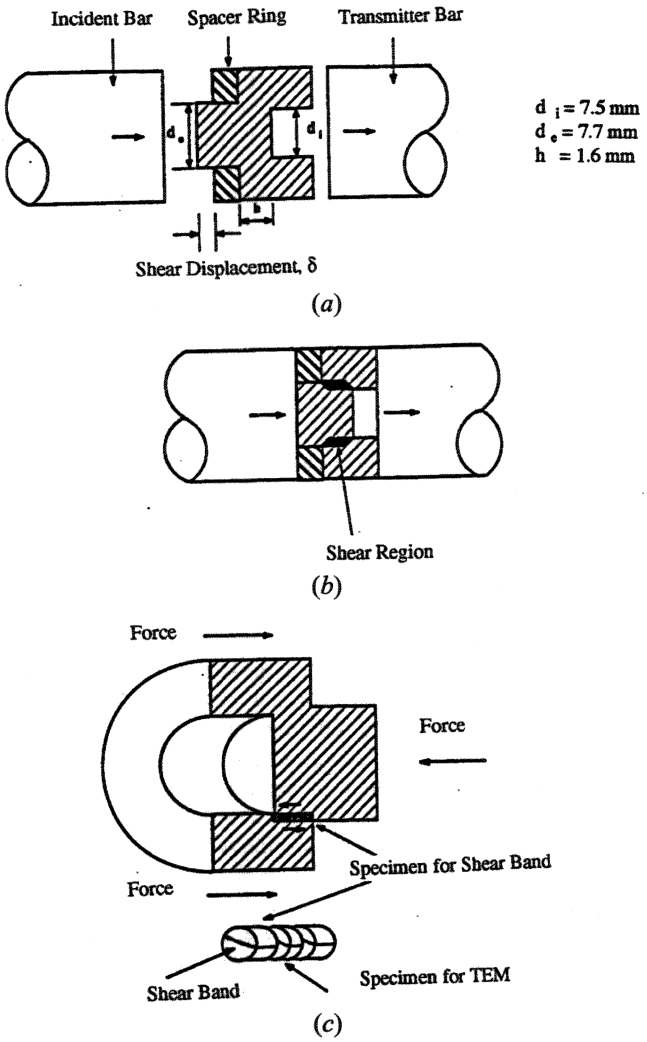

Fig. 4—Loading scheme of the hat-shaped specimen in the Hopkinson bar: (*a*) specimen before compression, (*b*) specimen after compression, and (*c*) extraction of specimen for transmission electron microscopy.

hat specimen, which were sliced as shown in Figure 3(c). The slices were ground and thinned. The best results were obtained with an electropolish solution containing 60 pct orthophosphoric acid and 40 pct water 273 K for a potential of 5 V.

III. RESULTS AND DISCUSSION

A. *Effect of Grain Size*

Compressive tests were conducted at room temperature on the annealed materials with four different grain sizes at strain rates of 10^{-4}, 10^{-3}, 10^{-1}, and 3×10^{3} s^{-1}. Figures 5(a) and (b) show the results for strain rates of 10^{-3} and 3×10^{3} s^{-1}, where it can be verified that the material strength increases as the grain size decreases. The effect of strain rate can be directly seen in Figure 6, which shows increasing strength with increasing strain rate for the grain size of 9.5 μm. An important effect of increasing the strain rate is to increase the work-hardening rate at a constant plastic strain. This phenomenon has been discussed by Klepaczko[31] and has received careful attention by Follansbee and Kocks[32] and Tong *et al.*[33] Tong *et al.* demonstrated that

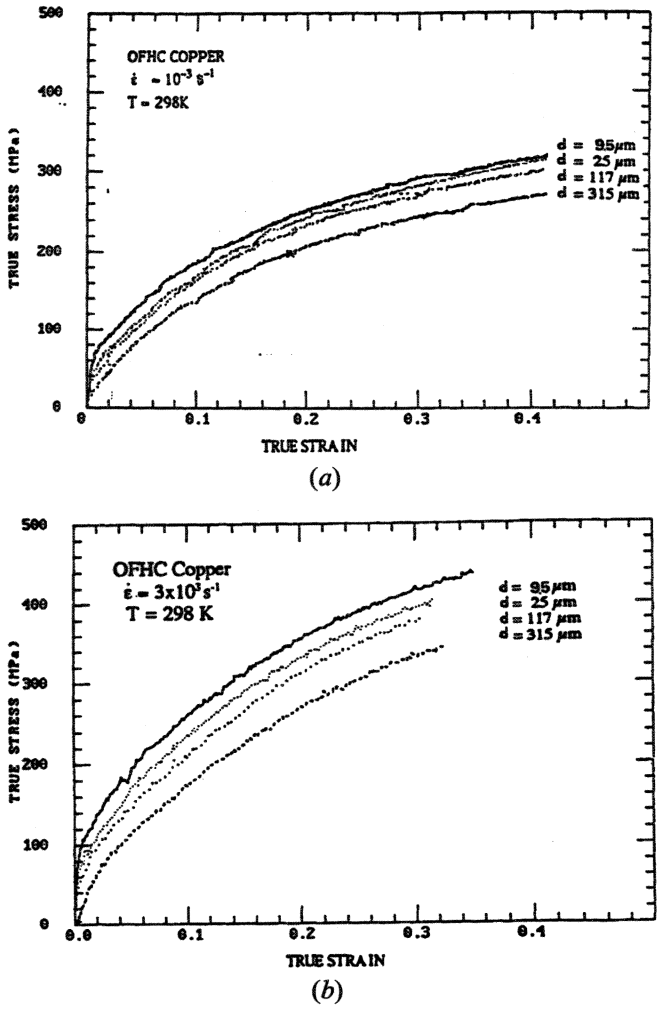

Fig. 5—Stress-strain curves for copper with different grain sizes: (*a*) strain rate of 10^{-3} s^{-1} and (*b*) strain rate of 3×10^{3} s^{-1}.

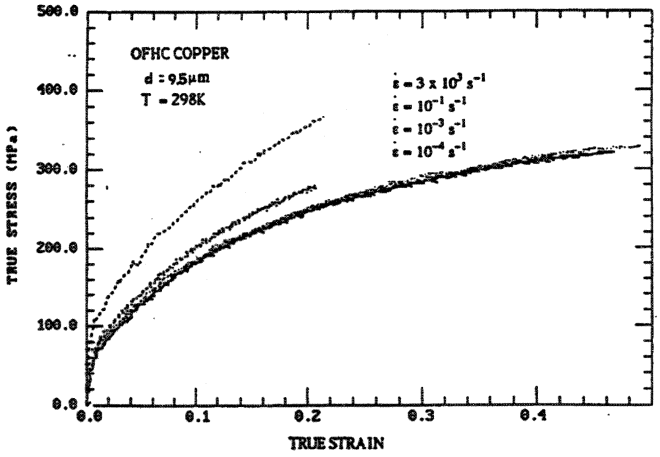

Fig. 6—Stress-strain curves for 9.5-μm grain-size copper deformed at different strain rates.

this strain-rate dependence of work hardening in copper is due to an increasing difficulty of dislocations to overcome obstacles at high strain rates, leading to an increased multiplication rate and to an increase in the strain-rate sensitivity of work hardening.

The reciprocal of the square root of grain size plotted *vs*

the flow stress represents the well-known Hall–Petch relationship:[34,35]

$$\sigma = \sigma_0 + k_S d^{-1/2} \quad [4]$$

where σ is the yield stress, σ_0 is a frictional stress required to move dislocations, k_S is a constant, and d is the grain size. A linear least-squares analysis of the data yields a slope for each line, k, which is the material sensitivity to grain-size strengthening. The values of k obtained in this investigation (0.56×10^{-4} to 2.6×10^{-4} GPa$\sqrt{\text{m}}$) compare favorably with literature values, where a significant scatter is found: Feltham and Meakin:[1] 3.53×10^{-4}; Gourdin and Lassila;[5,6] 2.78×10^{-4}; and Zerilli and Armstrong:[3] 1.58×10^{-4} GPa$\sqrt{\text{m}}$. Figures 7(a) and (b) show the Hall–Petch slopes as a function of strain and strain rate, respectively. At a low strain rate of 10^{-4} s^{-1}, a decrease in the slope from 1.72×10^{-4} to 0.56×10^{-4} GPa$\sqrt{\text{m}}$ is observed, with an increase in strain; the slope remains relatively constant around 2.60×10^{-4} GPa$\sqrt{\text{m}}$ for the high-strain-rate tests (8×10^3 s^{-1}). This is consistent with results by Gourdin and Lassila.[5,6]

The decrease in k with increasing strain at low strain rates suggests that other dislocation barriers, in addition to the grain boundaries, become progressively important at high strains. At very small plastic strains, inhomogeneity is pronounced due to differently oriented and shaped grains and to elastic anisotropy. Most of the plastic flow would then depend on the "geometrically necessary" dislocations, and in an initially annealed polycrystal, the slip length is about equal to the grain size. But, as the strain increases, hardening is dominated by the random interactions between dislocations, the "statistically stored" component. Therefore, the slip length decreases, taking on values lower than the grain size. Gracio *et al.*[36] investigated the effect of grain size on the substructural evolution in copper and found that, for larger grain sizes, the central region of grains exhibited a dislocation distribution characteristic of monocrystals. On the other hand, the compatibility conditions dictated a much more restricted response for dislocations. The larger grain sizes had a considerable linear hardening regime, whereas small grain sizes had parabolic hardening from the outset of plastic deformation. This can lead to a decrease in k_S, the grain size sensitivity of flow stress, with plastic strain. At high strain rates, the rate of dislocation multiplication is higher and other factors come into play. There is a greater tendency for mechanical twinning for the specimens with a large grain size, and this contributes to an increase in the work-hardening rate. This aspect will be discussed in Section B in connection with shock-induced hardening.

B. *Effect of Shock Loading*

The optical micrographs of the shocked copper specimens revealed significant differences with grain size, as shown in Figure 8. Whereas profuse twinning was observed for the larger grain sizes (117 and 315 μm), twinning was virtually absent for the 9.5-μm specimen. This profuse twinning, with an intertwin spacing of approximately 15 μm is more clearly evident in Figure 9. Transmission electron microscopy carried out with dark-field analysis using the matrix and twin reflections, shown in Figure 10, incontrovertibly identifies the features as twins. Figure 10(a)

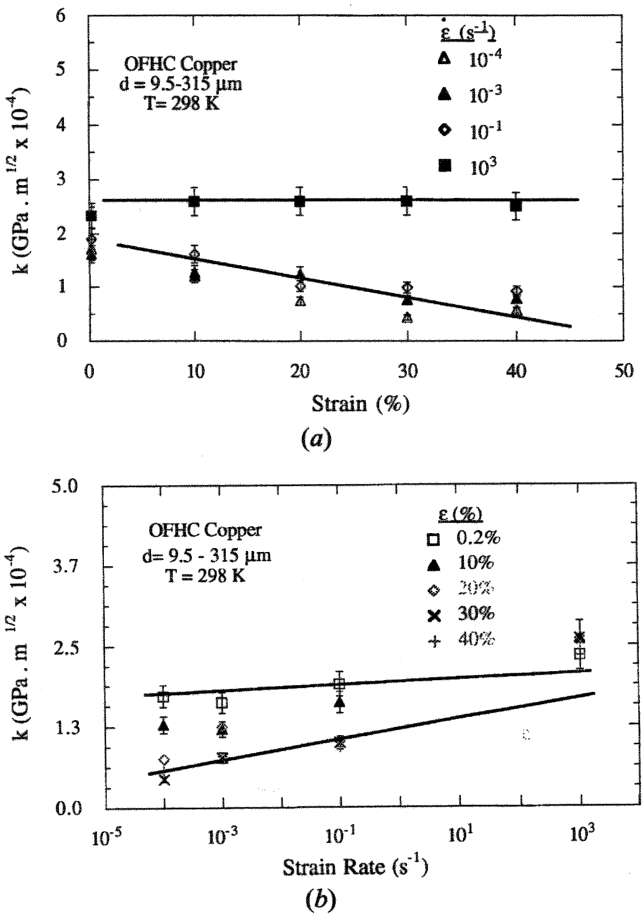

Fig. 7—Slopes of the Hall–Petch relationship: (*a*) as a function of strain and (*b*) as a function of strain rate.

presents the bright-field image, whereas Figures 10(c) and (d) show dark-field images of spots 1 and 2. This difference in shock response caused considerable concern and was the reason for repeating experiment 1 with greater care in recovery. The possibility that postshock heating could have contributed to the absence of twinning for the 9.5-μm specimen was eliminated when identical results were obtained for experiment 2.

The effect of shock loading in hardening the copper with different grain sizes is seen in Figures 11(a) and (b). The curves display the responses of the four different grain sizes for compressive tests at (a) low strain rate (10^{-3} s^{-1}) and (b) high strain rate (8000 s^{-1}). Clearly, the material with a grain size of 9.5 μm hardened much less than the one with 315 μm, showing that shock hardening was highly dependent on grain size. The work-hardening rate of the 315-μm grain-sized specimen is very low, whereas the smaller grain sizes exhibit significant hardening. The strain-rate dependence of flow stress is clearly seen by comparing Figures 11(a) and (b): the flow stress at 8×10^3 s^{-1} is approximately 25 pct higher than at 10^{-1} s^{-1}. These results are consistent with the unshocked material and with experimental results obtained by Gray and Follansbee[37] and Tong *et al.*[33] Figures 12(a) and (b) show the stress-strain response of materials with 9.5 and 315 μm, respectively, for different strain rates. The strength for both materials increased as the strain rate increased, and the overlapping

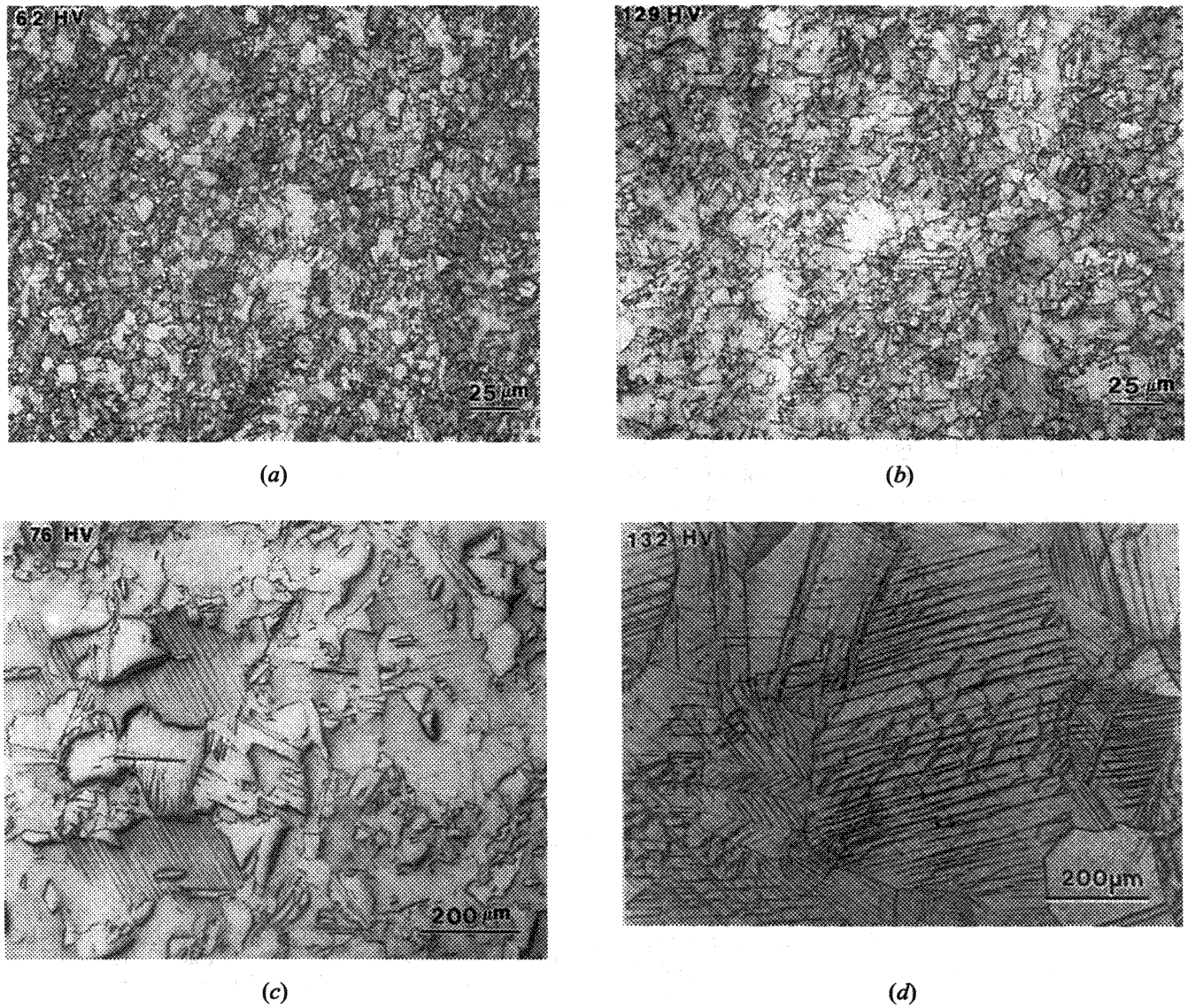

Fig. 8—Optical micrographs from shocked samples from experiment 2: (*a*) 9.5 μm, (*b*) 25 μm, (*c*) 117 μm, and (*d*) 315 μm; microhardness numbers are indicated in the upper left-hand corners.

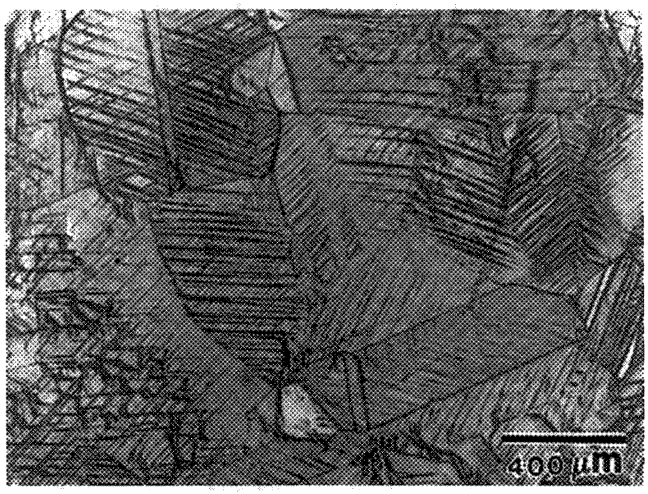

Fig. 9—Optical micrograph showing profuse twinning in shocked copper with 315 μm.

observed in the material with 315 μm for strain rates of 8000 and 2000 s^{-1} is due to oscillations in the curves.

Figures 13(a) and (b) show the stress-strain response of materials with grain sizes of 9.5 and 315 μm plotted with the origin of the shock-loaded specimens offset by the approximate total effective transient shock strain corresponding to a shock-loading pressure of 50 GPa. The effective strains undergone by the material at the shock front and release portion of the wave are of approximately equal magnitude and opposite senses. The total effective strain is expressed as

$$\varepsilon_{\text{total}} = \frac{4}{3} \ln \left(\frac{V}{V_0} \right) \qquad [5]$$

where V_0 and V are the initial and shock compressed volumes, respectively. This procedure was introduced by Meyers and Orava.[38] One may verify that the offset curve for 315 μm exhibits a flow stress considerably higher than the

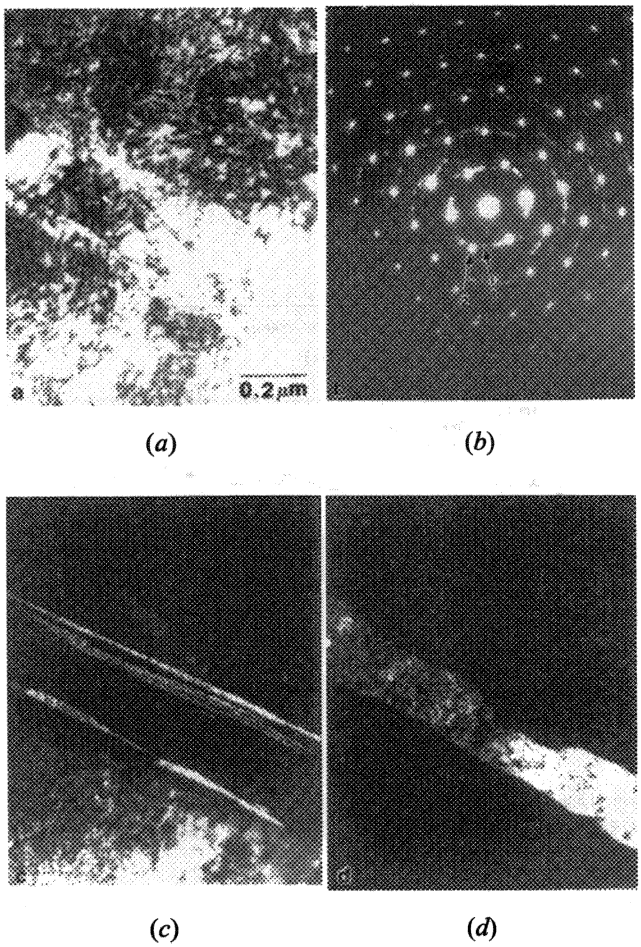

Fig. 10—Transmission electron micrographs showing deformation twinning in shocked copper: (*a*) bright field, (*b*) selected area electron diffraction pattern, (*c*) dark-field image from spot 1, and (*d*) dark-field image from spot 2.

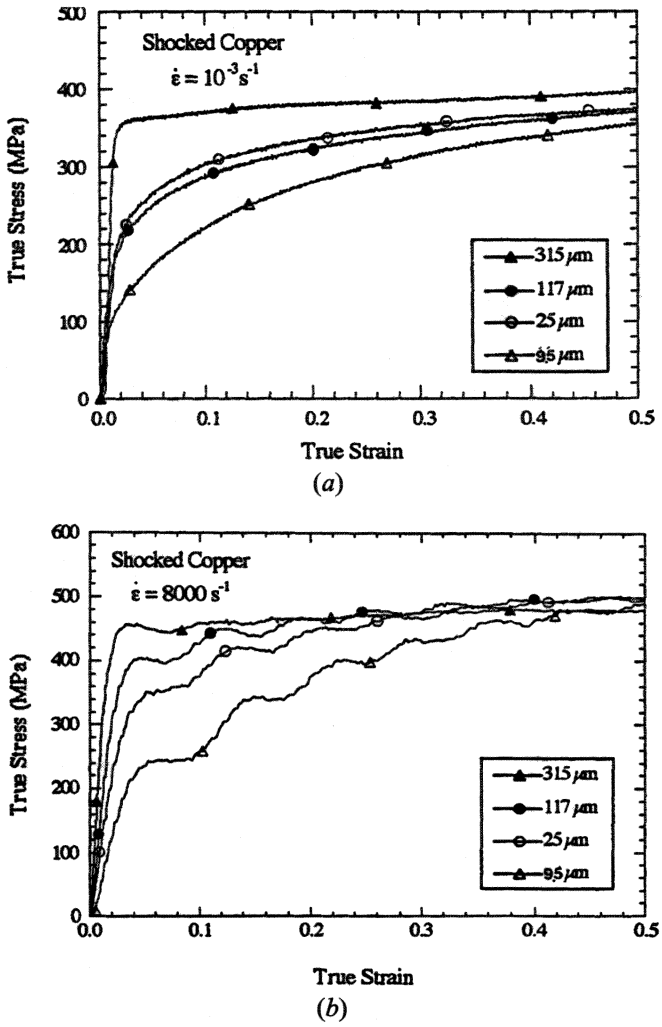

Fig. 11—Stress-strain curves of materials with (*a*) 9.5 μm and (*b*) 315 μm for different grain sizes: (a) 10^{-3} s^{-1} and (b) 8000 s^{-1}.

unshocked copper, which suggests that strain is not a state variable under these conditions. For the 9.5-μm grain size, the opposite occurs: the flow stress after shock loading is lower.

From thermodynamic predictions and experimental observations on residual temperatures generated by shock impact on copper, a pressure of 50 GPa can produce a residual temperature rise of 198 K.[39] This temperature is sufficiently high to produce changes in the shock-loaded microstructure. Recently, Haessner and Sztwiertnia[40] investigated microstructural aspects of the recrystallization of highly rolled pure copper. Using a temperature of 413 K for 10 minutes, they were able to achieve the initial stage of recrystallization. On the other hand, 1-minute isochronal annealing experiments conducted in a parallel study with a 70-μm grain-size copper showed that a temperature of 773 K was necessary to completely anneal the shocked material. Experiment 2 was carried out with additional precautions (precooling of specimens and quenching bath) in order to minimize the postshock recovery processes. In spite of all this additional care in the recovery experiments, the specimens from experiment 2 showed the same mechanical response as those of experiment 1, as shown in Figures 11 and 12. Therefore, it is concluded that the differences in response due to grain size effects are indeed the result of differences in microstructural changes effected by shock loading.

C. *The Effect of Grain Size on the Threshold Pressure for Twinning*

It is now necessary to examine the observation that the larger grain-size materials twin more readily than small grain-size ones. Kestenbach and Meyers[41] have investigated the residual microstructure and mechanical response of shock-loaded stainless steel (AISI-304) with four different grain sizes (23, 55, 85, and 187 μm). They found that the strengthening efficiency of shock loading decreased with increasing grain size and did not follow a simple Hall–Petch behavior. This study showed that grain-size effects can have a pronounced effect on the shock-induced substructure. Wongwiwat and Murr[42] attributed the grain-size dependence of twinning in shock loading of Mo to the possibility that the higher dislocation density associated with the smaller grained material could inhibit twinning. It is well known that the grain size has an effect on the twinning propensity of metals (*e.g.*, Mahajan and Williams,[43] Gray,[44] and Christian and Mahajan[45]). This is true both at low and high strain rates. At low strain rates, Marcinkowski and Lipsitt[46] observed, for Fe-3 pct Si at grain sizes above

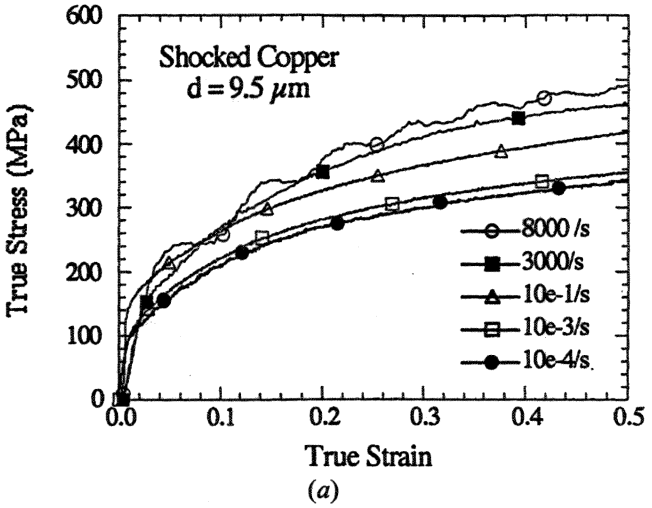

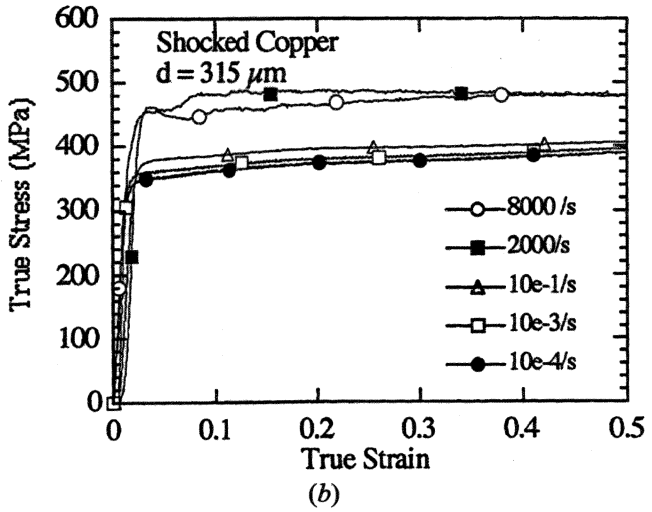

Fig. 12—Stress-strain curves of material with (*a*) 9.5 μm and (*b*) 315 μm for different strain rates.

30 μm, that plastic deformation was initiated by twinning. Owen and Hull[47] observed the same phenomenon for chromium. Armstrong and Zerilli[48] compiled experimental results at high and low strain rates for ARMCO* iron and showed that the Hall–Petch plots for slip and twinning intersect. Whereas this phenomenon is well known, it is not so well understood. Mahajan and Chin[49] made careful observations and were able to propose a complete mechanism, involving the splitting of [110] dislocations into three partials. The transmission of plastic deformation from one grain to the next is dependent on the stress concentrations at the grain boundaries which are, in turn, dependent on grain size.

*ARMCO is a trademark of Armco, Inc., Middletown, OH.

Armstrong and Worthington[50] developed a constitutive relation for deformation twinning in bcc metals. It was shown by Mahajan and Chin[49] that twinning is intimately connected with slip. The model of Armstrong and Worthington[50] is based on twin initiation and can be extended to fcc metals. This microslip generates dislocation pileups which are grain-size dependent. The local stress required to activate twinning, τ_T, is related to the externally applied

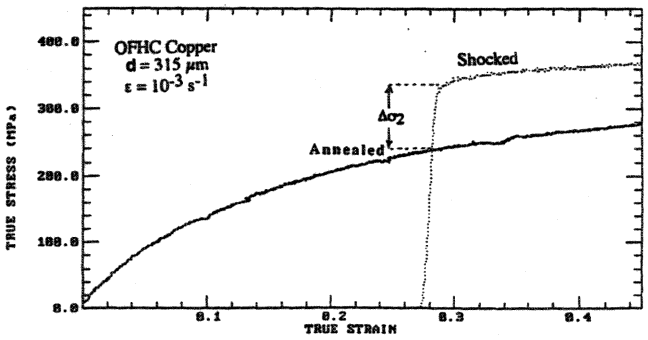

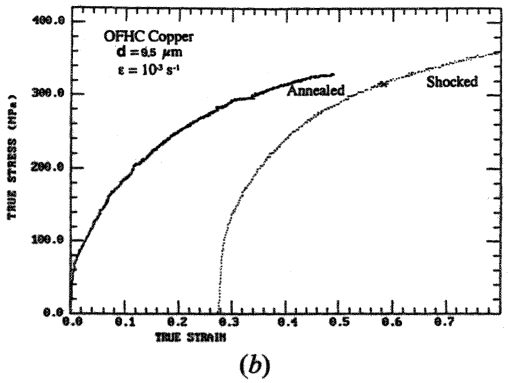

Fig. 13—Stress-strain curves of materials with (*a*) 9.5 μm and (*b*) 315 μm, plotted with the origin offset by the total transient shock strain.

stress, τ_e by

$$\tau_T \approx n_S \tau_e = C \frac{d}{G\mathbf{b}} \tau_e^2 \qquad [6]$$

$$\approx C \frac{d}{G\mathbf{b}} (\tau - \tau_0)^2 \qquad [7]$$

where C is a constant, n_s is the number of dislocations at a pileup (which is dependent on grain size, d), G is the shear modulus, **b** the burgers vector, and τ_0 a frictional shear stress. From Eq. [7],

$$\tau = \tau_0 + \left(\tau_T \frac{G\mathbf{b}}{C}\right)^{1/2} d^{-1/2} \qquad [8]$$

In terms of normal stress,

$$\sigma = \sigma_0 + m \left(\frac{\tau_T G\mathbf{b}}{C}\right)^{1/2} d^{-1/2} = \sigma_0 + k_T d^{-1/2} \qquad [9]$$

where

$$k_T = m\left(\frac{\tau_T G\mathbf{b}}{C}\right)^{1/2}$$

where m is an orientation factor (=0.5).

Armstrong and Worthington[50] compared the Hall–Petch slopes for slip, k_S (Eq. [4]), and twinning k_T (Eq. [9]) and found that

$$k_T \ . \ (1.5 - 7)\, k_S \qquad [10]$$

Macroslip and twinning can be considered as competitive mechanisms. Plastic flow will occur by either one or the other mechanism, whichever requires a lower stress. The

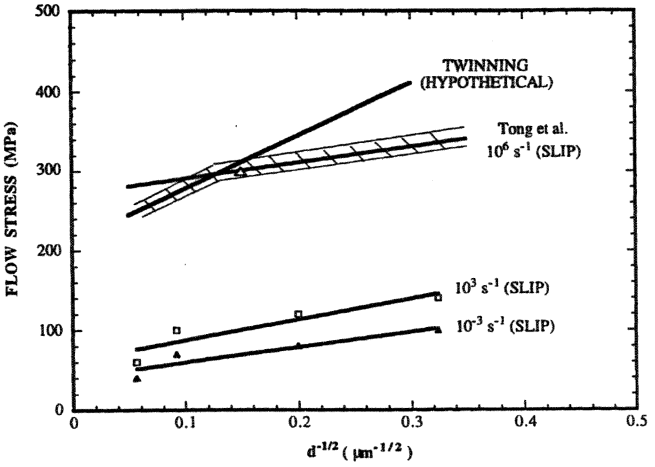

Fig. 14—Hall–Petch plots for plastic flow by slip (10^{-3}, 10^3, and 10^6 s^{-1}) and twinning (hypothetical), providing a rationale for twin-slip transition observed under shock compression.

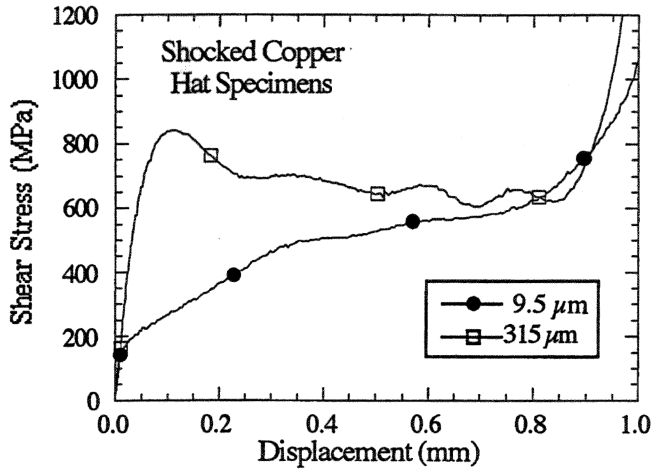

Fig. 15—Shear stress *vs* displacement curves obtained from hat-shaped specimen tests in a split Hopkinson bar at a strain rate of approximately 4×10^4 s^{-1} for materials with 9.5 and 315 μm.

graphical scheme proposed by Meyers and Murr[51] (Figure 20, p. 516) explains this.

A rationale that explains the propensity of large grain-size copper to exhibit twinning under shock-loading conditions consistent with the aforementioned discussion is provided in Figure 14. The Hall–Petch plots at 10^{-3} and 10^3 s^{-1} are shown to be parallel; a datum point by Tong *et al.*[33] provides the anchor for the relationship at 10^6 s^{-1}. It is assumed that the strain rate in shock loading is of this order of magnitude. Plastic flow by twinning is characterized by a slope k_T that is taken as $\sim 2\ k_S$. The intersection between the two lines was taken in accordance with the experimental observation of Figure 8: absence of twinning for the 9.5- and 25-μm grain sizes. Figure 13 provides a rationale for the switch from plastic flow by twinning to slip, under shock loading, when a critical grain size is reached. The Hall–Petch line for twinning is, according to Armstrong and Worthington,[50] only weakly dependent on strain rate and temperature, and therefore, one unique line is used to represent the entire response in Figure 13. The plot of Figure 13 is general and should explain the grain-size-induced slip-twinning transition under shock loading. A more detailed analysis will be presented later.[52]

D. *High-Strain, High-Strain-Rate Experiments*

1. *The effect of grain size on the threshold pressure for twinning*

Figure 15 shows the shear stress *vs* displacement curves obtained from hat-shaped specimens tested in a split Hopkinson bar at a shear strain rate of approximately 4×10^4 s^{-1}. While the 9.5-μm grain-size copper work hardens all the way up to the point where the spacer ring stops the shear, the material with 315 μm exhibits some work softening, with a clear drop of the shear stress from 800 MPa to about 600 MPa. These results are consistent with the compression test results of Figure 11, although the specimens were subjected to a high shear strain ($\gamma \sim 4$) in Figure 15.

Optical micrographs from the shear regions of hat-shaped specimens for both 9.5- and 315-μm materials are shown in Figure 16. There are significant differences between the shear deformation regions in the two materials. The band is diffuse in the material with the small grain size, exhibiting a width in some places larger than 300 μm. On the other hand, the material with the large grain size shows a well-localized shear band with a width smaller than 200 μm. The band has a very well-defined boundary for the 315-μm specimens, cutting across existing grains and eliminating all traces of the existing microstructure. Indeed, localization of plastic deformation for 9.5-μm specimens is forced by geometry and does not manifest itself by an alteration of the microstructure.

Armstrong,[53] among others, observed that deformation twinning can effectively strengthen a material. Twinning causes an effective decrease in slip barrier spacing, which reduces the linear dimensions over which internal stress concentrations may build up: an increased applied stress is required to initiate further plastic flow. Additionally, twinning brings into play auxiliary deformation systems that work harden the material in order to prevent the buildup of stress concentrations. The interfaces of deformation twins represent effective obstacles to slip. Murr[54] proposed that shock-induced deformation twins should act as a subgrain refinement, thereby following a Hall–Petch type relationship.

Thus, using k_S equal to 2.60×10^{-4} GPa$\sqrt{\text{m}}$ and taking d equal to the average intertwin space, which was found to be about 0.8 μm by transmission electron microscopy, a value of flow stress around 290 MPa is found. This can, undoubtedly, explain part of the strengthening of the material with larger grain size, with a flow stress of 350 MPa, shown in Figure 11. The remainder (350 to 290 MPa) can be explained through the known increase in dislocation density produced by shock loading.

2. *The onset of plastic instability*

A semiquantitative prediction of the instability strain required for shear band localization can be carried out through the instability criterion that has been used by Recht[55] and Culver:[56]

$$\frac{d\sigma}{d\varepsilon} \leq 0 \qquad [11]$$

This criterion can be used with the Johnson–Cook[57] equa-

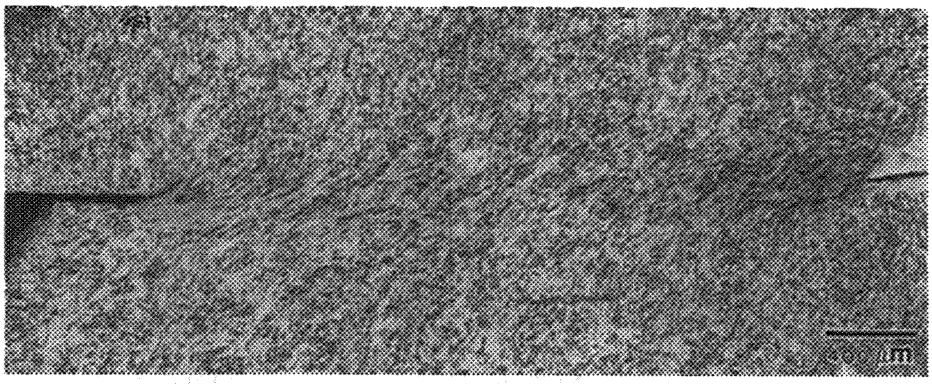

(*a*)

(*b*)

Fig. 16—Optical micrographs from the shear regions of hat-shaped specimens for (*a*) 9.5-μm and (*b*) 315-μm materials.

Table II. Parameters of the Johnson–Cook Equation for 9.5 and 315-μm Grain-Size Copper and Original Johnson–Cook Parameters[57]

	9.5 μm	315 μm	Johnson–Cook
σ_0	90 MPa	320 MPa	90 MPa
B	356 MPa	80 MPa	292 MPa
n	0.44	0.24	0.31
C	0.010	0.012	0.025
m	1	1	1.09

tion for the stress, σ, which is expressed as

$$\sigma = (\sigma_0 + B\varepsilon^n) \qquad [12]$$

$$\left(1 + C \ln \frac{\dot{\varepsilon}}{\dot{\varepsilon}_0}\right)\left[1 - \left(\frac{T - T_{\text{room}}}{T_{\text{melt}} - T_{\text{room}}}\right)^m\right]$$

where σ_0, B, n, C, $\dot{\varepsilon}_0$, and m are parameters and T, T_{room}, and T_{melt} are the test temperature, room temperature, and melting temperature, respectively. Assuming that 90 pct of the plastic deformation energy is converted to heat and combining Eqs. [11] and [12], the conversion of the plastic deformation energy into heat, though an adiabatic process, leads to the following expression:

$$nB\varepsilon^{n-1} = \frac{0.9\ m\ (1 + C \ln \varepsilon^*)}{PC_P\ (T_{\text{melt}} - T_{\text{room}})}\ (\sigma_0 + B\varepsilon^n)^2 \qquad [13]$$

where ρ is the density, C_P is the heat capacity, and $\dot{\varepsilon}^*$ is the normalized strain rate ($=\dot{\varepsilon}/\dot{\varepsilon}_0$). For simplicity, the thermal softening parameter, m, was taken as one. This is close to the value of 1.09 determined by Johnson and Cook.[57] No elevated temperature tests were conducted for these two grain-sized materials. The parameters of the Johnson–Cook equation obtained for these two conditions are shown in Table II. By applying these parameters to Eq. [13], the following instability strains were found:

$$d = 9.5\ \mu\text{m} \rightarrow \gamma_{\text{inst}} = 12.9$$
$$d = 315\ \mu\text{m} \rightarrow \gamma_{\text{inst}} = 2.3$$

Although these results are not rigorously quantitative, in view of the uncertainties in the strain rate and temperature dependence of flow stress and the nature of the curve-fitting exercise, they indicate that localization will occur earlier for the coarser grained specimen, which is consistent with the present experimental observations. The major difference between the two conditions is that significant work hardening occurs for the 9.5-μm grain size.

Transmission electron microscopy reveals the differences between the 9.5- and 315-μm grain-size specimens very clearly, as well as the microstructural evolution within the plastic deformation regions. The effects of shock on microstructure are well known and have been systematically documented by Murr,[54] among others. Dislocation cells are seen in Figure 17(a), while Figure 17(b) shows deformation twins and cells characteristic of the 315-μm specimen. The diameter of these cells (λ) at the imposed pressure (50 GPa) is consistent with the relationship predicted by Murr and Kuhlmann-Wilsdorf:[58]

$$\lambda \alpha P^{-1/2} \qquad [14]$$

(*a*)

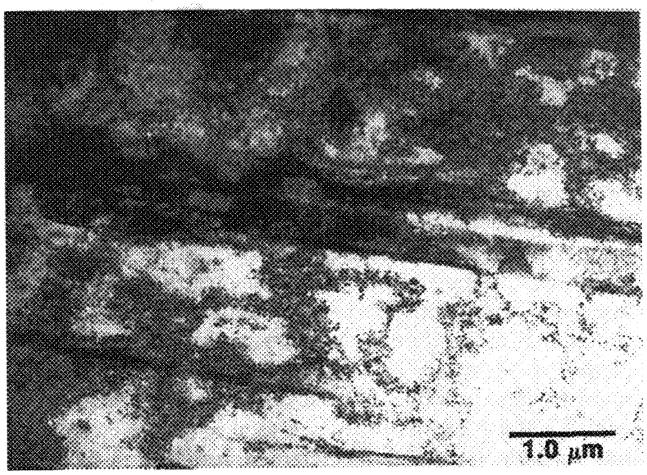

(*b*)

Fig. 17—Transmission electron micrograph of shocked copper with 315 μm: (*a*) cell structure and (*b*) deformation twins and cells.

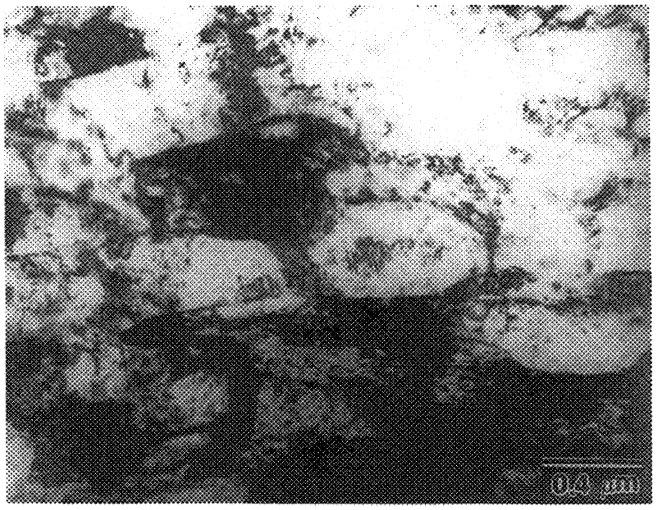

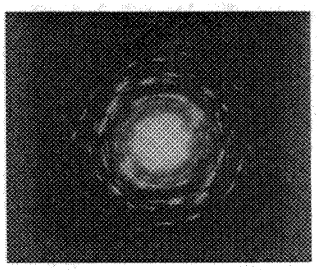

(*a*)

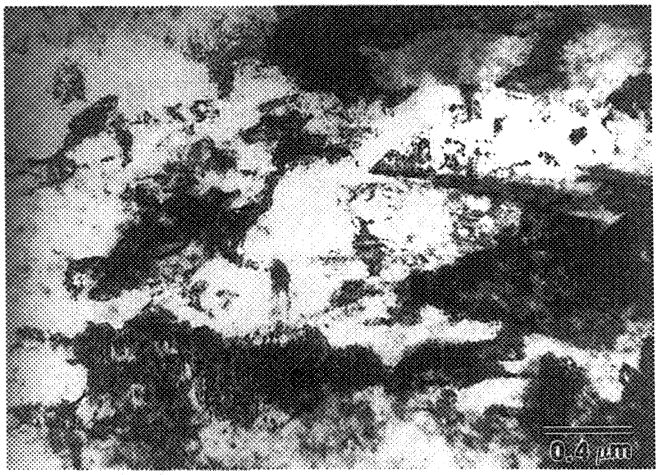

(*b*)

Fig. 18—Transmission electron micrographs from the shear region of the specimen with 315 μm showing (*a*) recrystallized microstructure composed of new recrystallized grains with approximately 0.2- to 0.5-μm diameter and (*b*) interface of shear localization region showing formation of micrograins.

where P is the pressure. As the shear band in the deformed specimen is approached, the equiaxed cells are replaced by elongated cells. Inside the shear band, these elongated cells break down and are replaced by small grains, with a relatively low dislocation density (Figure 18(a)). The grain boundaries are well defined. This microstructure is similar to the one observed earlier for a 70-μm grain-size specimen subjected to the same high-strain, high-strain-rate plastic deformation. It was attributed to dynamic recrystallization. The diffraction figure displays a well-defined ring pattern, indicating that the beam was imaging a multicrystal region. This recrystallization can explain the softening observed on hat-shaped specimen tests previously shown in Figure 15. Figure 18(b) shows the shear band interface where the micrograins are not yet completely formed. The mechanism for the formation of this recrystallized structure seems to be the same as the one observed for the 70-μm grain-size copper specimen subjected to similar deformation. Derby[59] classified dynamic recrystallization into migrational and rotational. No annealing twins are seen in the recrystallized grains, suggesting that the mechanism for their formation is a rotational one. Andrade *et al.*[20] describe the two alternative mechanisms in detail. This leads to the conclusion that intense plastic deformation under quasiadiabatic conditions produces a refinement of a 315-μm grain-size material to recrystallized grains of 0.2 to 0.5 μm, which explains the observed work softening observed in the mechanical tests. On the other hand, in the shear region in the material with 9.5-μm grain size, no recrystallization was observed. The shock-induced microstructure was composed of dislocation cells, with the cell walls somewhat better defined than for the 315-μm grain-size specimens. Figure 19(a) shows a grain boundary surrounded by dislocation cells. Within the intense plastic deformation region, the dis-

(*a*)

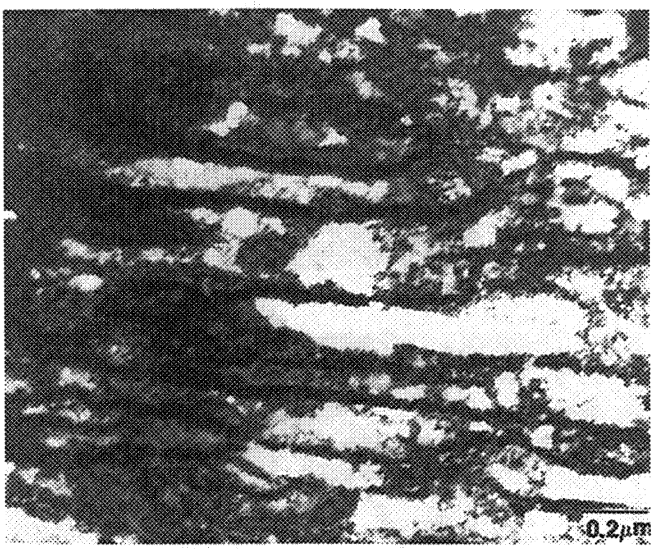

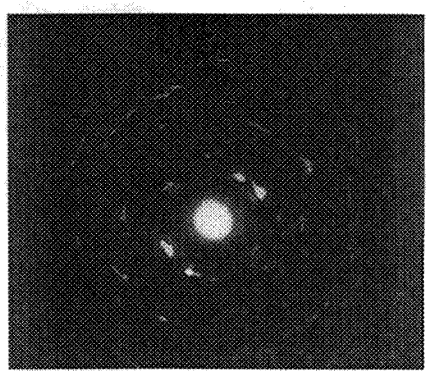

(*b*)

Fig. 19—Transmission electron micrograph from the specimen with 9.5 μm: (*a*) grain boundary surrounded by dislocation cells and (*b*) elongated cell from the shear region.

location cells became elongated, as shown in Figure 19(b). The greater work-hardening ability of the microstructure shown in Figure 19, as compared to the one shown in Figure 18, is responsible for a resistance to localization in the fine-grained material. Based on the flow stress-strain behavior of the shocked material, it is also clear that the temperature achieved at a constant strain, under adiabatic conditions, is lower for the 9.5-μm than for the 315-μm grain-size condition. Thus, the plastic strain at which the elongated cells break down and give rise to micrograins is lower for the latter (315 μm) condition.

IV. CONCLUSIONS

The shock and high-strain response of copper were established as a function of grain size. The low- and high-strain-rate responses of copper with different grain sizes are similar, confirming the work of Gourdin and Lassila.[5,6] However, the grain size has a profound effect on the shock response, and a shock pressure of 50 GPa generates profuse twinning for a 315-μm grain-size condition and virtually no twinning for 9.5-μm grain size. Postshock high-strain, high-strain-rate experiments reveal that the 9.5-μm grain-size copper hardens significantly, while the 315-μm grain-size copper does not. A rationale is proposed for the slip-twinning transition, based on differences in the Hall–Petch slope for these two competing plastic deformation mechanisms. This leads to localization of plastic deformation in the coarse-grained specimen, whereas the plastic deformation tends to be homogeneous for the 9.5-μm grain-size specimen. Within the plastic deformation region of the 315-μm specimen, at a shear strain of ~5, a structure consisting of small grains with low dislocation density is observed. This is indicative of dynamic recrystallization by a rotational mode. For the 9.5-μm specimen, no recrystallization is observed. This research shows that the residual microstructure of a fine-grain-sized shocked material should yield a better performance when used as a shaped-charged liner since the localization is retarded, resulting in increased time for fracture for the jet. Shear localization has been recently observed in copper explosively forged projectiles by Tang *et al.*[60] and with the use of the thick-walled cylinder by Nesterenko and Bondar.[61] This is an important effect, and this work demonstrates that the grain-size dependence of shock strengthening (through mechanical twinning at larger grain sizes) significantly affects shear band susceptibility. A rationale for this behavior is proposed, based on the intersection between the Hall–Petch lines for slip and twinning at high strain rates.

ACKNOWLEDGMENTS

We thank the United States Army Research Office University Research Initiative Program (Contract No. DAAL03-86-K-0169), the National Science Foundation (Grant No. MSS-9021671), the Brazilian Government through the National Council for Research, and the Office of Science and Technology of the Ministry of the Brazilian Army for support of this research. The shock loading experiments were conducted at the Energetic Materials Research and Testing Center, New Mexico Institute of Mining and Technology, and we thank Professor N.N. Thadhani and Mr. F. Sandstrom for their help with the shock-loading experiments. Mr. J. Isaacs provided valuable assistance and carried out a number of high-strain-rate experiments; his contribution is gratefully acknowledged. We thank Professor K.S. Vecchio for the transmission electron micrograph

of Figure 10 and for many useful discussions, which provided fruitful insights. The rolling of the copper was carried out by Dr. J. Beatty, United States Materials Technology Laboratory; his contribution is greatly appreciated.

REFERENCES

1. P. Feltham and J.D. Meakin: *Phil. Mag.*, 1957, vol. 2, p. 105.
2. S.L. Wang and L.E. Murr: *Metallurgy*, 1980, vol. 13, pp. 203-24.
3. F.J. Zerilli and R.W. Armstrong: *J. Appl. Phys.*, 1987, vol. 61, pp. 1816-25.
4. A.S. Shume, Y.J. Chang, and M.N. Bassim: *Mater. Sci. Eng.*, 1989, vol. A108, pp. 241-45.
5. W.H. Gourdin and D.H. Lassila: *Acta Metall. Mater.*, 1991, vol. 39, pp. 2337-48.
6. W.H. Gourdin and D.H. Lassila: *Mater. Sci. Eng.*, 1992, vol. A151, pp. 11-18.
7. A.H. Chokshi, A. Rosen, J. Karch, and H. Gleiter: *Scripta Metall.*, 1989, vol. 23 (10), pp. 1679-84.
8. C.G. Schmidt, Robert D. Caligiuri, Jacques H. Giovanola, and David C. Erlich: *Metall. Trans. A*, 1991, vol. 22A, pp. 2349-57.
9. M.P. Bondar' and V.F. Nesterenko: *J. Phys. IV*, 1991, vol. 1 (c3), pp. 163-70.
10. V.F. Nesterenko, M.P. Bondar', and I.V. Ershov: in *High-Pressure Science and Technology—1993*, S.C. Schmitt, J.W. Shaner, G.A. Samara, and M. Ross, eds., AIP Press, New York, NY, 1994, pp. 173-76.
11. U.R. Andrade: Ph.D. Thesis, University of California, San Diego, CA, 1993.
12. U.R. Andrade, M.A. Meyers, A.H. Chokshi, and K.S. Vecchio: *J. Phys. IV*, 1994, vol. 4 (c8), pp. 361-66.
13. W.P. Walters and J.A. Zukas: *Fundamentals of Shaped Charges*, Wiley Interscience, New York, NY, 1989, p. 2.
14. M. Lichtenberger, M. Scharf, and A. Bohman: Report No. CO 218/81, French-German Research Institute, Saint-Louis, France, (ISL), Sept. 1981.
15. W.H. Gourdin: in *Shock-Wave and High-Strain-Rate Phenomena in Materials*, M.A. Meyers, L.E. Murr, and K.P. Staudhammer, eds., Marcel Dekker, New York, NY, 1992, pp. 597-609.
16. W.H. Gourdin: in *Shock-Wave and High-Strain-Rate Phenomena in Materials*, M.A. Meyers, L.E. Murr, and K.P. Staudhammer, eds., Marcel Dekker, New York, NY, 1992, pp. 611-16.
17. A.C. Gurevitch, L.E. Murr, W.W. Fisher, S.K. Varma, A.H. Advani, and L. Zernow: *Mater. Charact.*, 1993, vol. 30, pp. 201-16.
18. M.A. Meyers, L.W. Meyer, J. Beatty, U.R. Andrade, K.S. Vecchio, and A.H. Chokshi: in *Shock-Wave and High-Strain-Rate Phenomena in Materials*, M.A. Meyers, L.E. Murr, and K.P. Staudhammer, eds., Marcel Dekker, New York, NY, 1992, pp. 529-42.
19. A.H. Chokshi and M.A. Meyers: *Scripta Metall. Mater.*, 1990, vol. 24, pp. 605-10.
20. U.R. Andrade, M.A. Meyers, K.S. Vecchio, and A.H. Chokshi: *Acta Metall. Mater.*, 1994, vol. 42, pp. 3183-95.
21. R.E. Reed-Hill and R. Abbaschian: *Physical Metallurgy Principles*, PWS-Kent, Boston, 1992, pp. 250 and 259.
22. I.M. Ghauri, M.Z. Butt, and S.M. Raza: *J. Mater. Sci.*, 1990, vol. 25, pp. 4782-84.
23. M.A. Mogilevsky and L.A. Teplyakova: in *Metallurgical Applications of Shock-Wave and High-Strain Rate Phenomena*, L.E. Murr, K.P. Staudhammer, and M.A. Meyers, eds., Marcel Dekker, 1986, pp. 419-27.
24. G.T. Gray III: in *High Pressure Shock Compression of Solids*, J.R. Asay and M. Shahinpoor, eds., Springer-Verlag, New York, NY, 1993, pp. 187-215.
25. P.S. DeCarli and M.A. Meyers: in *Shock-Wave and High-Strain-Rate Phenomena in Metals*, M.A. Meyers and L.E. Murr, eds., Plenum Press, New York, NY, 1981, pp. 341-73.
26. K.-H. Hartmann, H.-D. Kunze, and L.W. Meyer: in *Shock Waves and High-Strain-Rate Phenomena in Metals*, M.A. Meyers and L.E. Murr, eds., Plenum Press New York, NY, 1981, pp. 325-37.
27. L.W. Meyer and S. Manwaring: in *Metallurgical Applications of Shock-Wave and High-Strain-Rate Phenomena*, L.E. Murr, K.P. Staudhammer, M.A. Meyers, eds., Marcel Dekker, New York, NY, 1986, pp. 657-74.
28. H. Kolsky: *Proc. R. Soc. B*, 1949, vol. 62, pp. 676-700.
29. S. Nemat-Nasser, J.B. Isaacs, and J.E. Starrett: *Proc. R. Soc. London A*, 1991, vol. 435, pp. 371-91.
30. S. Nemat-Nasser, J.B. Isaacs, G. Ravichandran, and J.E. Starrett: *Proc. of TTCP Workshop on New Techniques of Small Scale High Strain Rate Studies*, Australia, 1989, p. 343.
31. J.R. Klepaczko: *J. Phys.*, 1988 vol. 49 (c3), pp. 553-60.
32. P.S. Follansbee and U.F. Kocks: *Acta Metall.*, 1988, vol. 36, pp. 81-93.
33. W. Tong, R.J. Clifton, and S. Huang: *J. Mech. Phys. Solids*, 1992, vol. 40, pp. 1251-94.
34. E.O. Hall: *Proc. R. Soc.*, 1951, vol. B64, pp. 742-53.
35. N.J. Petch: *J. Iron Steel Inst.*, 1953, vol. 174, pp. 25-28.
36. J.J. Gracio, J.V. Fernandes, and J.H. Schmitt: *Mater. Sci. Eng.*, 1989, vol. A118, pp. 97-105.
37. G.T. Gray III and P.S. Follansbee: in *Impact Loading and Dynamic Behavior of Materials*, C.Y. Chiem, H.D. Kunze, and L.W. Meyer, eds., Informationsgellsshaft, Verlag, Germany 1988, p. 541-548.
38. Marc A. Meyers and R. Norman Orava: *Metall. Trans. A*, 1976, vol. 7A, pp. 179-90.
39. R.G. McQueen and S.P. Marsh: *J. Appl. Phys.*, 1960, vol. 31, p. 253.
40. F. Haessner and K. Sztwiertnia: *Scripta Metall.*, 1992, vol. 27, pp. 1545-50.
41. H.J. Kestenbach and Marc A. Meyers: *Metall. Trans. A*, 1976, vol. 7A, pp. 1943-50.
42. K. Wongwiwat and L.E. Murr: *Mater. Sci. Eng.*, 1978, vol. 35, pp. 273-85.
43. S. Mahajan and D.E. Williams: *Int. Metall. Rev.*, 1973, vol. 18, pp. 43-61.
44. G.T. Gray III: in *Encyclopedia of Material Science and Engineering*, Pergamon Press, Oxford, United Kingdom, 1990, suppl., vol. 2, pp. 859-66.
45. J.W. Christian and S. Mahajan: in *Progress in Materials Science*, 1995, in press.
46. M.J. Marcinkowski and H.A. Lipsitt: *Acta Metall.*, 1962, vol. 10, p. 95.
47. W.S. Owen and D. Hull: in *Refractory Metals and Alloys II*, M. Semdryshen and I. Perlmutter, eds., Interscience, New York, NY, 1963, p. 1.
48. R.W. Armstrong and F.J. Zerilli: *J. Phys.*, 1988, vol. 49 (c3), pp. 529-34.
49. S. Mahajan and G.Y. Chin: *Acta Metall.*, 1973, vol. 21, pp. 1353-63.
50. R.W. Armstrong and P.J. Worthington: in *Metallurgical Effects at High Strain Rates*, R.W. Rohde, B.M. Butcher, J.R. Holland, and C.H. Karnes, eds., Plenum Press, New York, NY, 1973, pp. 401-14.
51. M.A. Meyers and L.E. Murr: in *Shock Waves and High-Strain Rate Phenomena in Metals*, M.A. Meyers and L.E. Murr, eds., Plenum Press, New York, NY, 1981, pp. 487-530.
52. M.A. Meyers and V.F. Nesterenko: in preparation (1995).
53. R.W. Armstrong: in *Deformation Twinning*, R.E. Reed-Hill, J.P. Hirth, and H.C. Rogers, eds., Gordon and Breach Science Publications, New York, NY, 1964, p. 356.
54. L.E. Murr: in *Shock Waves and High-Strain-Rate Phenomena in Metals*, M.A. Meyers and L.E. Murr, eds., Plenum Press, New York, NY, 1981, pp. 607-673.
55. R.F. Recht: *J. Appl. Mech.*, 1964, vol. 31, pp. 189-93.
56. R.S. Culver: in *Metallurgical Effects at High Strain Rates*, R.W. Rohde, B.M. Butcher, J.R. Holland, and C.H. Karnes, eds., Plenum Press, New York, NY, 1973, pp. 519-30.
57. G.R. Johnson and W.H. Cook: in *Proc. 7th Int. Symp. on Ballistics*, The Hague, The Netherlands, 1983, pp. 541-47.
58. L.E. Murr and D. Kuhlmann-Wilsdorf: *Acta Metall.*, 1978, vol. 26, pp. 847-57.
59. B. Derby: *Acta Metall. Mater.*, 1991, vol. 39, pp. 955-62.
60. N.Y. Tang, P. Niessen, R.J. Pick, and M.J. Worswick: *Mater. Sci. Eng.*, 1991, vol. A131, pp. 153-60.
61. V.F. Nesterenko and M.P. Bondar: *DYMAT J.*, 1994, vol. 1, pp. 245-51.